Comparative Study of the Efficiency of Rectangular and Triangular Flat Plate Solar Collectors through Finite Element Method

Estudio Comparativo de la Eficiencia de Colectores Solares de Placa Plana Rectangular y Triangular mediante el Método de Elementos Finitos

I. Simbaña[1]   🆔 0000-0002-3324-3071   W. Quitiaquez[2]   🆔 0000-0001-9430-2082

P. Cabezas[2]   🆔 0000-0001-5114-6913   P. Quitiaquez[2]   🆔 0000-0003-0472-7154

[1]Instituto Superior Universitario Sucre, Grupo de Investigación en Ingeniería Mecánica y Pedagogía de la Carrera de Electromecánica (GIIMPCEM), Quito, Ecuador
E-mail: isimbana@tecnologicosucre.edu.ec

[2]Universidad Politécnica Salesiana, Grupo de Investigación en Ingeniería, Productividad y Simulación Industrial (GIIPSI), Quito, Ecuador
E-mail: wquitiaquez@ups.edu.ec, ecabezasg@est.ups.edu.ec, rquitiaquez@ups.edu.ec

Abstract

This investigation compared the efficiency of a flat-plate solar collector with triangular and square geometry, by using the finite element method (FEM). The design of the geometries and the utilized parameters for the simulation were obtained from previous publications. SolidWorks was used to model the two collectors, meanwhile, the Fluent module of the ANSYS software was used for the simulation by the FEM. Collectors integrated a pipe of 7 mm internal diameter with a plate thickness of 11 mm; the defined material was aluminum. The experiment was conducted under ambient conditions at a temperature of 20 °C, accompanied by a solar radiation intensity of 1000 W·m^{-2}. The heat transfer surfaces employed were $61\ 250 \text{ mm}^2$ for the triangular collector and $122\ 500 \text{ mm}^2$ for the square collector. The quality of the mesh was excellent, obtaining a skewness of 0.2486, with which efficiencies of 62 and 39 % and maximum temperatures of 27 and 25.5 °C were obtained for the triangular and square collectors, respectively. Due to the geometries performing as fins, the temperatures are higher in the corners and, therefore, achieving higher efficiency is impossible.

Resumen

En esta investigación, se comparó la eficiencia de un colector solar de placa plana con geometría triangular y cuadrada, a través del enfoque del método de elementos finitos (FEM, por sus siglas en inglés), se llevó a cabo la simulación. Las geometrías y los parámetros empleados en la simulación fueron extraídos de investigaciones previamente publicadas. Se utilizó el software SolidWorks para el modelado de los dos colectores, mientras que el módulo Fluent del software ANSYS fue utilizado para la simulación por el método FEM. Para los colectores se utilizó una tubería de 7 mm de diámetro interno, con un espesor de placa de 11 mm y de aluminio. Se consideró temperatura ambiente de 20 °C, con una radiación solar de 1000 W·m^{-2} y superficies de transferencia de calor $61\ 250$ y $122\ 500 \text{ mm}^2$ para el colector triangular y cuadrado, respectivamente. La calidad del mallado fue excelente, alcanzando *skewness* de 0.2486. De esta manera, luego del proceso de simulación se obtuvo eficiencias de 62 y 39 % y temperaturas máximas de 27 y 25.5 °C para el colector triangular y cuadrado, respectivamente. Debido a que las geometrías actúan como aletas, las temperaturas son más altas en las esquinas y por esto no es posible alcanzar mayor eficiencia.

Index terms— Solar collector, flat-plate, efficiency, FEM.

Palabras clave— Colector solar, placa plana, eficiencia, FEM.

1. INTRODUCTION

The existing problems of environmental changes worldwide have been derived from the consumption of fossil fuels, which is the main dominant in the energy matrix worldwide [1]. The elevated consumption has led to a rapid surge in the levels of carbon dioxide (CO_2). This has led to a crisis of distribution, production, and consumption of energy, causing the scarcity of this fossil resource [2]. To mitigate the effects of environmental changes, the International Atomic Energy Agency (IAEA) and the Kyoto Protocol have proposed the use of renewable sources, which is accepted by developed countries [3]. This suggestion has spurred the development of fresh concepts involving the implementation of inventive prototypes aimed at alleviating the repercussions of high-consumer demand of fossil resources. [4].

Solar energy is the world's most abundant energy resource, provided by nature providing clean energy [5]. The photovoltaic cell converts solar energy into electricity through the use of doped semiconductors [6]. Extensive literature exists on the characterization of the cell or solar cell, as outlined below. The application of solar collectors has been evolving by proposing new models, such as Ion et al. [7] presented, a new flat plate thermal solar collector for the integration of facades. The numerical analysis considered a triangular geometry collector, modeling it in SolidWorks as design software and ANSYS to identify deformation and stagnation points. Three solar collectors with absorber plates in black, green, and orange hues were produced, yielding efficiencies of 55, 42, and 35 %, respectively.

The numerical and experimental investigation of a triangular storage collector was carried out by Ahmed [8]. As collectors are suitable devices for use in heating water, they are applied for domestic and industrial purposes. Andrade et al. [9] developed a systematic investigation for hours in the summer and winter seasons with and without a hot water outlet. Their experimental results showed that the efficiency during winter and summer at maximum temperatures was 48.7 % at 65 °C and 62.2 % at 70 °C, respectively. Moss et al. [10] affirm that collectors must be designed to be used in cold conditions, on cloudy days, or with high supply temperatures, to achieve maximum efficiency. The authors have deduced that the enhanced efficiency of solar collectors is attributed to the decrease in internal pressure, necessitating values below 0.5 Pa.

When comparing the efficiency of a solar collector based on ANSYS Fluent results with experimental data, it becomes evident that the inflow into the storage collector should occur at the bottom of the coldest section. Simultaneously, the outflow from the storage collector should be positioned at the top of the collector's coldest section [11]. By considering the literature review carried out and that has been taken as a reference, for the development of this investigation, Table 1 presents a brief description of the most relevant publications, which used a flat-plate solar collector.

Table 1: Investigations carried out on flat collectors

Parameter	Efficiency [%]	Water as the working fluid	Coating	Max. Temp. [°C]
Ion et al. [7]	55	X	X	80
Ahmed [8]	62.2			
Moss et al. [10]			X	
Fathabadi [12]	74.9	X		
Saffarian et al. [13]		X		
Müller et al. [14]		X	X	16.5
Fan et al. [15]	69.4	X		

The aim of this work is the geometric comparison between triangular and square solar collectors. For this, the obtained data, the efficiencies, and the maximum temperatures were contrasted, which can be reached with the constant solar irradiation flow of 1 000 $W \cdot m^{-2}$. This document is organized as described below, Materials and Methods present the parameters of each collector, as well as the mathematical modeling necessary to support the investigation. In Results, the obtained graphs for each geometry with the simulation software are compared. Finally, in the Conclusions, the obtained results are discussed and the presented information is summarized.

2. MATERIALS AND METHODS

2.1 Conceptualization of the design

Solar collectors are mechanisms used to gather, impregnate, and transfer solar energy to a fluid, which can be water or air. They can also be utilized to heat water, for heating systems, or heating swimming pools [16]. Among the types of renewable energy, solar is very prominent, due to the use of photovoltaic cells and collectors to produce electricity and water heating, respectively, in industrial processes or integrated systems of homes [17]. Solar collectors are used for various applications and different utilities, trying to take better advantage of the use of solar energy. Therefore, a different geometry of a solar collector is proposed, considering the design presented by Ion et al. [7]. Fig. 1a shows a triangular solar collector, to compare the efficiencies against a square collector, as shown in Fig. 1b.

The central body consists of an aluminum cavity that will be located under the absorbent plate of the collector through which water, as working fluid, will circulate. Fig. 2 shows the cross-section used for both geometrics, where the absorber plate contained in a box is displayed.
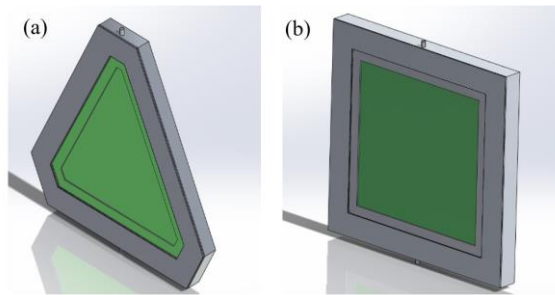
Figure 1: Solar collector (a) triangular, (b) square
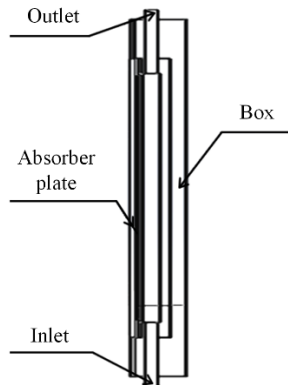
Figure 2: Collector cross-section

The central body consists of an aluminum cavity that will be located under the absorbent plate of the collector through which water, as working fluid, will circulate. Being made of corrosion-resistant aluminum material, it will allow hot water to be used for any need that the user requires. When used for the facades of buildings or houses, coatings must be placed to obtain an architectural design. For the joining and sealing elements, rubber is applied between the aluminum cavities and the absorbent plate [18]. The design needs to use not very thick absorber plates to take advantage of the heat transfer to the fluid since thick plates absorb a lot of heat and not all of this heat is transferred to the fluid [19].

2.2   Solar thermal collector model

The triangular and square collector models were designed in SolidWorks, resembling the measurements in the article by Ion et al. [7]. The simulation was carried out in ANSYS Fluent, in which, the input conditions are presented in Table 2.

Table 2: Parameters utilized in the simulation

Parameter	Symbol	Units	Value
Tilt angle	β	-	0
Ambient temperature	T_a	°C	20
Absorber plate thermal conductivity	k	W·m^{-1}·K^{-1}	237
Specific flow rate	$\dot{m}$	kg·m^{-1}·s^{-1}	0.02
Absorber plate emissivity	ε_p	-	0.115
Absorber plate temperature	T_p	°C	20 - 100
Solar irradiation	G	W·m^{-2}	1000

For the design of the collectors, both triangular and square, only the geometry sketch was considered. It allows to parameterize the simulation and obtain the required results. The velocity was determined in relation to a specific flow rate of 0.02 kg·m^{-2}·s^{-1} and irradiance ranging from 800 to 900 W·m^{-2} [7]. Under these conditions, there is a favorable trend towards elevating the temperature from 20 °C to approximately 60 °C.

In Fig. 3, the schematic of the triangular solar collector is depicted, with the water inlet marked in blue at a temperature of 20 °C. The central section of the collector corresponds to the region where the working fluid will circulate. At the top, there is the outlet of the working fluid that has been heated. The proposed square solar collector also complies with the same schematic characteristics as the triangular solar collector.
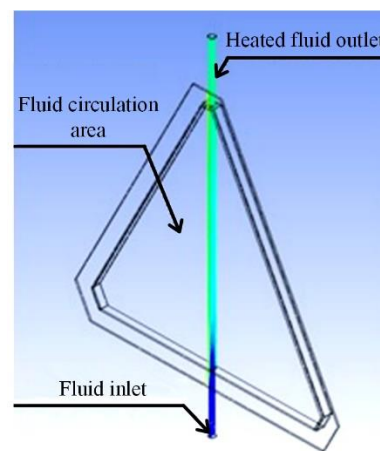
Figure 3: Triangular solar collector scheme

Table 3 details the parameters that both triangular and square solar collectors share, with similar characteristics.

Table 3: Characteristics of triangular and square solar collectors

Characteristics	Triangular	Square
Length [mm]	350	350
Height [mm]	350	350
Pipe diameter [mm]	7	7
Transfer area [mm^2]	61 250	122 500
Distance of the inlet pipe [mm]	80	80
Width [mm]	11	11
Material	Aluminum	Aluminum

2.3   Mathematical modeling of the flat-plate solar collector

In flat-plate solar collectors, regardless of geometry, the amount of solar radiation absorbed by the collector is an important factor [12]. The received solar heat (Q_{in}) for a flat plate collector is expressed with equation (1):

$$Q_{in} = A_c \cdot G \qquad (1)$$

Where Ac is the collector area and G is the solar irradiation. Equation (2) is employed to calculate the

useful heat (Q_u) within the solar collector, considering the circulation of the working fluid within the collector, as detailed by Diez et al. [20]:

$$Q_u = A_c \cdot \dot{m} \cdot c_p (T_{out} - T_{in}) \qquad (2)$$

Where $\dot{m}$ is the mass Flow rate, c_p is the specific heat for water, T_{out} and T_{in} are the water temperature at the inlet and outlet, respectively. The global coefficient of heat loss (U_L) is a variable taken into account during the design phase of solar collectors. Anca et al. [21] have used equation (3), which expresses the sum of the loss coefficients:

$$U_L = U_t + U_b + U_e \qquad (3)$$

The higher loss coefficient (U_t) is obtained in the glazing due to the convection of heat and radiation that takes place in the absorber plate and as the radiation loss from the external glass plate to the environment. Wang et al. [22] use equation (4):

$$U_t = \left(\frac{1}{h_{c,p-c} + h_{r,p-c}} + \frac{1}{h_w + h_{r,c-a}} \right)^{-1} \qquad (4)$$

The convective heat coefficient ($h_{c,p-c}$) from the cover glass and absorber plate can be calculated by Deshmukh et al. [23] from equation (5):

$$h_{c,p-c} = N_u \cdot \frac{k}{L} \qquad (5)$$

Where L is the characteristic length and k is the thermal conductivity of the material. The Nusselt number (N_u) can be determined based on the Rayleigh number and the inclination angle, ranging from 0 to 75° taking into account its operation in a natural convection [24], through the application of equation (6):

$$N_u = 1 + 1.44 \cdot \left[1 - \frac{1708(\sin 1.8 \cdot \beta)^{1.6}}{R_a \cdot \cos \beta} \right] \cdot \left[1 - \frac{1708}{R_a \cdot \cos \beta} \right]$$
$$\cdot \left[\left(\frac{R_a \cdot \cos \beta}{5830} \right)^{\frac{1}{3}} - 1 \right] \qquad (6)$$

Where β is the Coefficient of thermal expansion. The Rayleigh number (R_a) is calculated by Robles-Campos et al. [25] by applying equation (7):

$$R_a = \frac{g \cdot \beta \cdot \Delta T \cdot L^3}{n} \qquad (7)$$

Where g is gravity. The radiation coefficient from the absorber plate to the cover ($h_{c,p-c}$) is derived using the equation (8):

$$h_{r.p-c} = \frac{\sigma \cdot (T_p^2 + T_c^2) \cdot (T_p + T_c)}{\frac{1}{\varepsilon_p} + \frac{1}{\varepsilon_c} - 1} \qquad (8)$$

Where ε is the emissivity. For the calculation of the radiation coefficient of the outer cover ($h_{r,p-c}$), Gunjo et al. [26] applied equation (9):

$$h_{r.c-a} = \varepsilon_c \cdot \sigma \cdot (T_p^2 + T_c^2) \cdot (T_p + T_c) \qquad (9)$$

The background loss coefficient caused by heat conduction (U_b) is calculated with equation (10):

$$U_b = \frac{k_b}{L_b} \qquad (10)$$

Mustafa et al. [27] calculated the border loss coefficient (U_ε) due to heat conduction by using equation (11):

$$U_\varepsilon = \frac{(U \cdot A) \cdot \varepsilon}{A} \qquad (11)$$

To obtain the efficiency of the collectors, the following relationships are applied [28]. Equation (12) allows to obtain the thermal power ($\dot{Q}$) of heat output from the collector, which is expressed as follows:

$$\dot{Q} = \dot{m} \cdot c_p \cdot (T_{out} - T_{in}) \qquad (12)$$

Finally, the relation of the equation (13) has been used by Xu et al. [29] for the direct calculation of the efficiency of the solar collector:

$$\eta = \frac{\dot{Q}}{G} \cdot 100\% \qquad (13)$$

2.4 ANSYS Software Equations

2.4.1 Energy

Quitiaquez et al. [30] conceptualize that the most important and powerful scientific laws are the conservation laws, in which, energy is a constant that is conserved in the universe. Therefore, it is declared that energy is neither created nor destroyed, it is only transformed. Equation (14) expresses the energy conversation equation to carry out a steady-state thermal analysis [31]:

$$\frac{\partial}{\partial t}(\rho \cdot E) + \nabla \cdot (\vec{u}(\rho \cdot E \cdot P)) =$$
$$\nabla \cdot [\lambda eff \cdot \nabla T - \Sigma h_k \cdot J_k] + S_E \qquad (14)$$

2.4.2 Energy Radiation

Solar energy represents an essentially limitless source of power, serving as a foundation for the creation of projects centered around this renewable alternative. This type of analysis considers radiative heat transfer, which is the transfer of thermal energy via electromagnetic waves. Mohamad et al. [32] articulated the representation of solar radiation in equation (15):

$$\nabla \cdot (I(\vec{r}, \vec{s})\vec{s}) + (a + \sigma_s) \cdot I \cdot (\vec{r}, \vec{s}) =$$
$$an^2 \cdot \frac{\sigma \cdot T^4}{\pi} + \frac{\sigma_s}{4\pi} \int_0^{4\pi} I \cdot (\vec{r}, \vec{s}) \cdot \Phi \cdot (\vec{r}, \vec{s}) \cdot d\Omega \qquad (15)$$

Where $\vec{r}$ and $\vec{s}$ representes the position and direction vectors, a and σ_s are the absorption scattering coefficients, respectively. I is the solar intensity, n is the refractive index, T is the ambient temperature and Ω is the solid angle. And for heat transfer by radiation, the Stefan-Botlzmann constant (σ) is 5.669 x 10^{-8} W·m^{-2}·K^{-4}.

2.5 Meshing

The finite element method allows the structural model to be perfected, creating an iteration process by applying a level of precision that ensures adequate convergence of the process. If the guarantee of this process is not

adequate, the quality of the results in the analysis of the design will be poor, granting a convergence of the non-optimal solution [33].

The mesh metric presents the information of nodes and elements, hence, the selection of a good mesh quality provides a better accuracy in the convergence of the solution in the simulation. For an excellent mesh, it is found in the values of 0 to 0.25 and for a lousy mesh surrounds the range of 0.98 to 1.00 [34]. Based on the aforementioned parameters and selecting a method of dominant tetrahedra, the metric of the triangular and square solar collector designs is performed by a selection of the mesh that is approximately in a range of 0.2486. Fig. 4a and Fig. 4b presents the discretization for the triangular and square collectors, respectively.
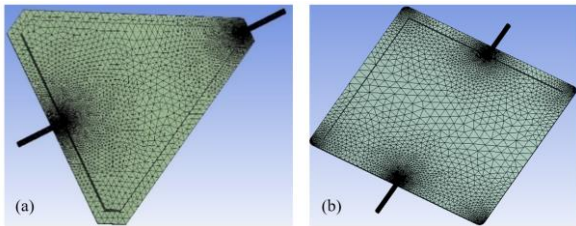
Figure 4: Mesh of solar collectors (a) triangular, (b) square

3. RESULTS

Fig. 5a and Fig. 5b present the temperature contours, therefore, it is possible to predict the behavior that the collectors will have throughout the increase in the flow of solar irradiation. The fluid initiates with an inlet temperature of approximately 20 °C, and the outlet temperature is monitored as the fluid exits the collectors.
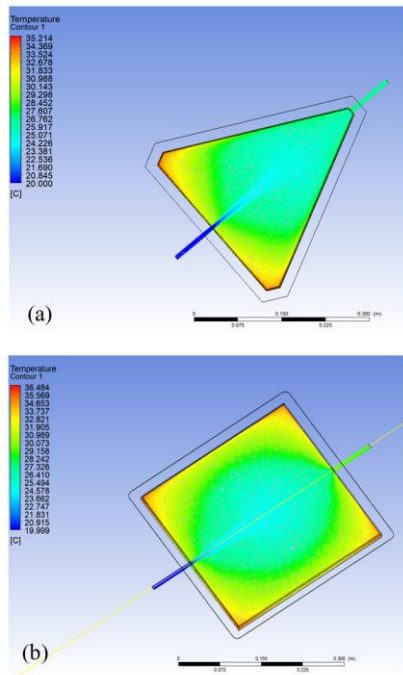
Figure 5: Heat distribution of solar collectors (a) triangular, (b) square

In Fig. 6a, the temperature trend graph of the working fluid originates at 20 °C, tracing the path of the triangular collector until it reaches an outlet temperature of 25.5 °C. Similarly, in the square solar collector illustrated in Fig. 6b, the identical trend line is apparent, albeit with the distinction that the working fluid's outlet temperature is 27 °C. Consequently, when compared to the temperature of the triangular collector, a notable difference is evident between the two geometries.
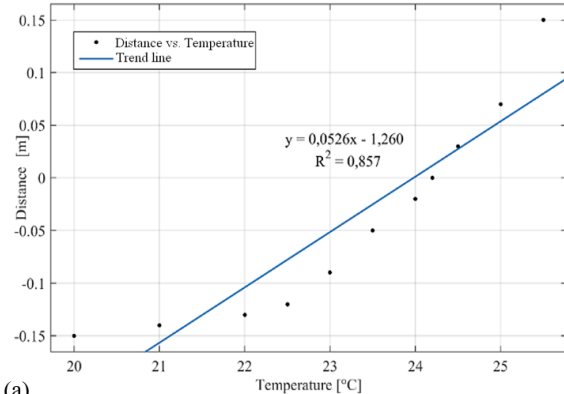
(a)
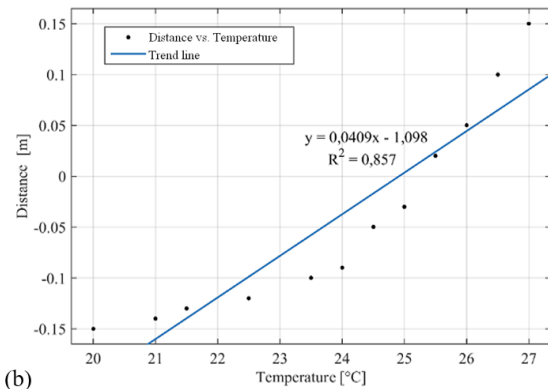
(b)

Figure 6: Working fluid temperature along the solar collectors (a) triangular, (b) square

The trend lines illustrate a proportional relationship between temperature and distance. Consequently, the forecast includes the maximum temperature that the working fluid is anticipated to reach based on the solar irradiation flux and the heat transfer area of each collector. The linear correlation coefficient R^2 serves as an indicator of the model's fit [35] and in the simulation, the obtained data exhibits a value of 85 %, signifying the proportion of variability in temperature increase relative to the distance covered by the working fluid. This figure suggests a reasonably acceptable reliability in the correlation between the data.

The calculation of the efficiency, equations (13) and (14) are applied, in which the thermal power of the collectors is calculated. It describes a tendency of the efficiency as a function of the temperature. Fig. 7a illustrates the performance of the triangular collector, depicting the efficiency trend. The highest efficiency is achieved at a maximum temperature of 62 %, occurring

at 25.5 °C. The square collector had an efficiency of 39 % at 27 °C and a cause for this very high variation in efficiency and temperature could be due to the geometry of each collector, as shown in Fig. 7b. The heat transfer areas of the absorber plate of both the square collector and the triangular collector are wider.

(a)

(b)
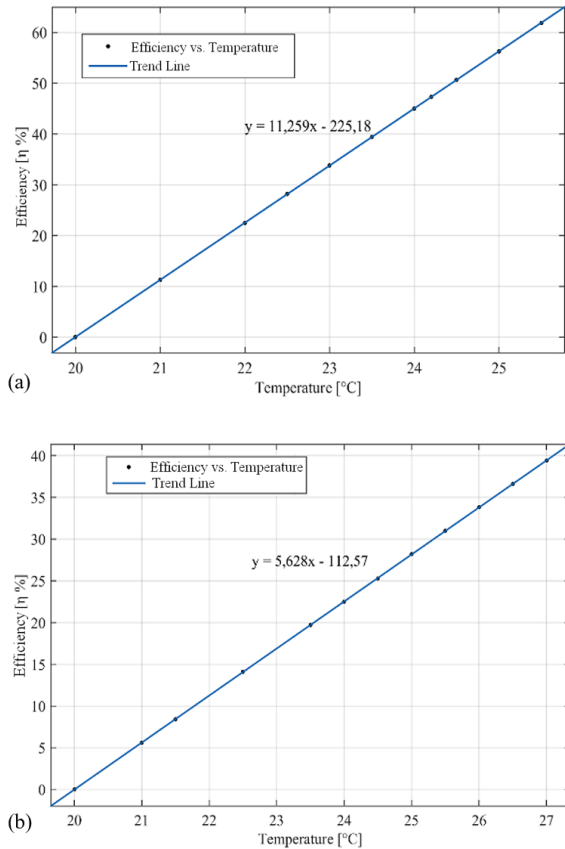
Figure 7: Working fluid temperature along the solar collectors (a) triangular, (b) square

The designs put forth in this research were developed by considering the geometry of an actual rectangular solar collector, which served as the basis for subsequent modifications. Moldovan et al. [36] conducted CFD simulations aimed at optimizing the efficiency of a triangular solar collector, taking layer thickness into account. They achieved an average efficiency of 55 %, and with a mass flow of 0.01 kg·s^{-1} and a 5 mm thickness, the maximum efficiency reached 66.12 %. Similarly, Noghrehabadi et al. [37] explored the efficiency of a square solar collector using both water and a nanofluid with silicon oxide as working fluids. The incorporation of nanofluid significantly enhanced the collector's efficiency, exceeding 50 %, while the use of water resulted in efficiency variations between 30 and 50 %, considering variations in mass flow and incident solar radiation. The efficiency outcomes for the proposed geometries align with those found in the literature, validating their credibility. However, further investigation is warranted to optimize the design, taking into consideration a more in-depth analysis of other variables associated with efficiency.

Fig. 8 presents the comparison of the efficiencies between both solar collectors that start from the same temperature of 20 °C. The efficiency of the solar collectors changes as the temperature increases, reaching a great difference in efficiency of 23 % between the collectors. The efficiency of the triangular solar collector closely mirrors the efficiency of the model introduced by Ion et al. [7], the first one to propose a collector with these characteristics. A triangular solar collector may potentially exhibit higher efficiency owing to its capacity to capture solar radiation from broader angles throughout the day, particularly at varying latitudes. Moreover, the triangular geometry can provide a larger surface area for absorption in a specific orientation when compared to a square collector. Comprehensive evaluations through computational simulations and experimental tests are essential to assess and compare the efficiency of various solar collector geometries in specific contexts.
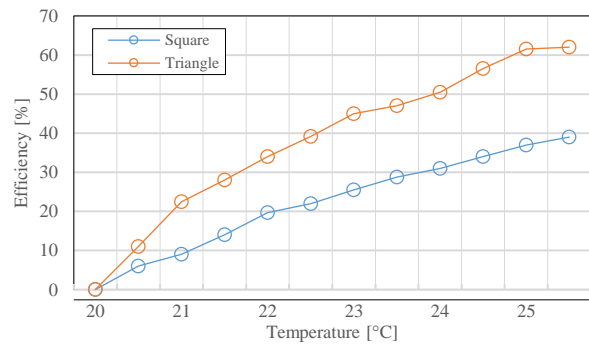
Figure 8: Comparison of the efficiencies of the triangular and square solar collectors

4. CONCLUSIONS

The efficiency comparison of the triangular and square solar collectors was analyzed. Modeling was designed in SolidWorks and simulations were carried out in ANSYS Fluent, obtaining a mesh skewness of 0.2486. The triangular collector demonstrates notable efficiency in converting solar radiation into usable heat, with 62 % of the incident radiation being effectively converted into thermal energy. In contrast, the square solar collector exhibits a lower efficiency, signifying a less effective conversion of only 39% of the incident solar radiation into thermal energy. Temperature reaches maximum values for square and triangular solar collectors of 27 and 25.5 °C, respectively. The material utilized for the design of the solar collectors is aluminum which has a high thermal conductivity. Finally, the collector behavior was analyzed with a color scale figure, which shows that higher temperatures tend to concentrate in the corners of the collectors. Therefore, a certain amount of heat will be discarded and for this reason, it is not possible to have higher levels of efficiency. Attaining an optimal design that maximizes the capture of solar radiation while minimizing thermal losses can pose challenges, and the process of optimization frequently demands a thorough, application-specific strategy.

5. REFERENCES

[1] P. Zeppini and J. C. J. M. van den Bergh, "Global competition dynamics of fossil fuels and renewable energy under climate policies and peak oil: A behavioural model," Energy Policy, vol. 136, p. 110907, 2020, doi: https://doi.org/10.1016/j.enpol.2019.110907.

[2] V. A. Ballesteros-Ballesteros and A. P. Gallego-Torres, "Modelo de educación en energías renovables desde el compromiso público y la actitud energética," Revista Facultad de Ingeniería, vol. 28, no. 52, pp. 27–42, Jun. 2019, doi: 10.19053/01211129.v28.n52.2019.9652.

[3] S. F. Razmi, B. Ramezanian Bajgiran, M. Behname, T. E. Salari, and S. M. J. Razmi, "The relationship of renewable energy consumption to stock market development and economic growth in Iran," Renew Energy, vol. 145, pp. 2019–2024, 2020, doi: https://doi.org/10.1016/j.renene.2019.06.166.

[4] J. E. Camacho-Quintana, J. E. Salamanca-Céspedes, and A. P. Gallego-Torres, "Induction Generator Characterization for a Medium and Low Wind-Power Generator," Revista Facultad de Ingenieria, vol. 29, no. 54, 2020, doi: 10.19053/01211129.v29.n54.2020.10900.

[5] A. A. Adenle, "Assessment of solar energy technologies in Africa-opportunities and challenges in meeting the 2030 agenda and sustainable development goals," Energy Policy, vol. 137, p. 111180, 2020, doi: https://doi.org/10.1016/j.enpol.2019.111180.

[6] M. Mikati, M. Santos, and C. Armenta, "Modelado y Simulación de un Sistema Conjunto de Energía Solar y Eólica para Analizar su Dependencia de la Red Eléctrica," Revista Iberoamericana de Automática e Informática Industrial RIAI, vol. 9, no. 3, pp. 267–281, 2012, doi: https://doi.org/10.1016/j.riai.2012.05.010.

[7] I. Visa, M. Moldovan, and A. Duta, "Novel triangle flat plate solar thermal collector for facades integration," Renew Energy, vol. 143, pp. 252–262, 2019, doi: https://doi.org/10.1016/j.renene.2019.05.021.

[8] O. K. Ahmed, "A numerical and experimental investigation for a triangular storage collector," Solar Energy, vol. 171, pp. 884–892, 2018, doi: https://doi.org/10.1016/j.solener.2018.06.097.

[9] A. X. Andrade Cando, W. Quitiaquez Sarzosa, and L. F. Toapanta, "CFD Analysis of a solar flat plate collector with different cross sections," Enfoque UTE, vol. 11, no. 2, pp. 95–108, Apr. 2020, doi: 10.29019/enfoque.v11n2.601.

[10] R. Moss, S. Shire, P. Henshall, F. Arya, P. Eames, and T. Hyde, "Performance of evacuated flat plate solar thermal collectors," Thermal Science and Engineering Progress, vol. 8, pp. 296–306, 2018, doi: https://doi.org/10.1016/j.tsep.2018.09.003.

[11] M. H. Alkhafaji, B. Freegah, and M. H. Alhamdo, "Effect of riser-pipe cross section and plate geometry on the solar flat plate collector's thermal efficiency under natural conditions," Journal of Engineering Research, Jul. 2023, doi: 10.1016/J.JER.2023.100141.

[12] H. Fathabadi, "Novel low-cost parabolic trough solar collector with TPCT heat pipe and solar tracker: Performance and comparing with commercial flat-plate and evacuated tube solar collectors," Solar Energy, vol. 195, pp. 210–222, 2020, doi: https://doi.org/10.1016/j.solener.2019.11.057.

[13] M. R. Saffarian, M. Moravej, and M. H. Doranehgard, "Heat transfer enhancement in a flat plate solar collector with different flow path shapes using nanofluid," Renew Energy, vol. 146, pp. 2316–2329, 2020, doi: https://doi.org/10.1016/j.renene.2019.08.081.

[14] S. Müller, F. Giovannetti, R. Reineke-Koch, O. Kastner, and B. Hafner, "Simulation study on the efficiency of thermochromic absorber coatings for solar thermal flat-plate collectors," Solar Energy, vol. 188, pp. 865–874, 2019, doi: https://doi.org/10.1016/j.solener.2019.06.064.

[15] M. Fan et al., "A comparative study on the performance of liquid flat-plate solar collector with a new V-corrugated absorber," Energy Convers Manag, vol. 184, pp. 235–248, 2019, doi: https://doi.org/10.1016/j.enconman.2019.01.044.

[16] W. Quitiaquez et al., "Análisis del rendimiento termodinámico de una bomba de calor asistida por energía solar utilizando un condensador con recirculación," Revista Técnica "energía," vol. 16, no. 2, pp. 111–125, Jan. 2020, doi: 10.37116/REVISTAENERGIA.V16.N2.2020.358.

[17] I. Reinier et al., "The Selection of a Solar Collector to Increase the Temperature of the Water Supply to the Steam Generator at the University of Cienfuegos. [Online]. Available: http://rus.ucf.edu.cu/

[18] N. H. Abu-Hamdeh, A. Khoshaim, M. A. Alzahrani, and R. I. Hatamleh, "Study of the flat plate solar collector's efficiency for sustainable and renewable energy management in a building by a phase change material: Containing paraffin-wax/Graphene and Paraffin-wax/graphene oxide carbon-based fluids," Journal of Building Engineering, vol. 57, p. 104804, Oct. 2022, doi: 10.1016/J.JOBE.2022.104804.

[19] E. Bellos and C. Tzivanidis, "A detailed investigation of an evacuated flat plate solar collector," Appl Therm Eng, vol. 234, p. 121334, Nov. 2023, doi: 10.1016/J.APPLTHERMALENG.2023.121334.

[20] F. J. Diez, L. M. Navas-Gracia, A. Martínez-Rodríguez, A. Correa-Guimaraes, and L. Chico-Santamarta, "Modelling of a flat-plate solar collector using artificial neural networks for different working fluid (water) flow rates," Solar Energy, vol. 188, pp. 1320–1331, 2019, doi: https://doi.org/10.1016/j.solener.2019.07.022.

[21] I. Visa et al., "Design and experimental optimisation of a novel flat plate solar thermal collector with trapezoidal shape for facades integration," Appl Therm Eng, vol. 90, pp. 432–443, 2015, doi: https://doi.org/10.1016/j.applthermaleng.2015.06.0 26.

[22] D. Wang et al., "Comparative analysis of heat loss performance of flat plate solar collectors at different altitudes," Solar Energy, vol. 244, pp. 490–506, Sep. 2022, doi: 10.1016/J.SOLENER.2022.08.060.

[23] K. Deshmukh, S. Karmare, and P. Patil, "Experimental investigation of convective heat transfer performance of TiN nanofluid charged U-pipe evacuated tube solar thermal collector," Appl Therm Eng, vol. 225, p. 120199, May 2023, doi: 10.1016/J.APPLTHERMALENG.2023.120199.

[24] M. Carmona and M. Palacio, "Thermal modelling of a flat plate solar collector with latent heat storage validated with experimental data in outdoor conditions," Solar Energy, vol. 177, pp. 620–633, Jan. 2019, doi: 10.1016/J.SOLENER.2018.11.056.

[25] H. R. Robles-Campos, B. J. Azuaje-Berbecí, C. J. Scheller, A. Angulo, and F. Mancilla-David, "Detailed modeling of large scale photovoltaic power plants under partial shading conditions," Solar Energy, vol. 194, pp. 485–498, Dec. 2019, doi: 10.1016/J.SOLENER.2019.10.043.

[26] D. G. Gunjo, V. K. Yadav, D. K. Sinha, I. E. Elseesy, G. M. Sayeed Ahmed, and M. A. H. Abdelmohimen, "Development and performance evaluation of solar heating system for biogas production process," Case Studies in Thermal Engineering, vol. 39, p. 102438, Nov. 2022, doi: 10.1016/J.CSITE.2022.102438.

[27] J. Mustafa, S. Alqaed, and R. Kalbasi, "Challenging of using CuO nanoparticles in a flat plate solar collector- Energy saving in a solar-assisted hot process stream," J Taiwan Inst Chem Eng, vol. 124, pp. 258–265, Jul. 2021, doi: 10.1016/J.JTICE.2021.04.003.

[28] J. J. Fiuk and K. Dutkowski, "Experimental investigations on thermal efficiency of a prototype passive solar air collector with wavelike baffles,"

Solar Energy, vol. 188, pp. 495–506, Aug. 2019, doi: 10.1016/J.SOLENER.2019.06.030.

[29] R. J. Xu, Y. Q. Zhao, H. Chen, Q. P. Wu, L. W. Yang, and H. S. Wang, "Numerical and experimental investigation of a compound parabolic concentrator-capillary tube solar collector," Energy Convers Manag, vol. 204, p. 112218, Jan. 2020, doi: 10.1016/J.ENCONMAN.2019.112218.

[30] W. Quitiaquez, J. Estupiñán-Campos, C. Nieto-Londoño, and P. Quitiaquez, "CFD Analysis of Heat Transfer Enhancement in a Flat-Plate Solar Collector/Evaporator with Different Geometric Variations in the Cross Section," Energies (Basel), vol. 16, no. 15, p. 5755, Aug. 2023, doi: 10.3390/en16155755.

[31] I. Simbaña, W. Quitiaquez, J. Estupiñán, F. Toapanta-Ramos, and L. Ramírez, "Evaluación del rendimiento de una bomba de calor de expansión directa asistida por energía solar mediante simulación numérica del proceso de estrangulamiento en el dispositivo de expansión," Revista Técnica "energía," vol. 19, no. 1, pp. 110–119, Jul. 2022, doi: 10.37116/REVISTAENERGIA.V19.N1.2022.524.

[32] S. T. Mohammad, H. H. Al-Kayiem, M. A. Aurybi, and A. K. Khlief, "Measurement of global and direct normal solar energy radiation in Seri Iskandar and comparison with other cities of Malaysia," Case Studies in Thermal Engineering, vol. 18, p. 100591, 2020, doi: https://doi.org/10.1016/j.csite.2020.100591.

[33] E. Nadal, J. J. Ródenas, E. M. Sánchez-Orgaz, S. López-Real, and J. Martí-Pellicer, "Sobre la utilización de códigos de elementos finitos basados en mallados cartesianos en optimización estructural," Revista Internacional de Métodos Numéricos para Cálculo y Diseño en Ingeniería, vol. 30, no. 3, pp. 155–165, 2014, doi: 10.1016/j.rimni.2013.04.009.

[34] J. G. Ardila-Marín, D. A. Hincapié-Zuluaga, and J. A. Sierra-del-Rïo, "Independencia de malla en tubos torsionados para intercambio de calor: caso de estudio," Revista de la Facultad de Ciencias, vol. 5, no. 1, pp. 124–140, Jan. 2016, doi: 10.15446/rev.fac.cienc.v5n1.54231.

[35] J. Manuel Rachel Him, L. A. Ortega, and J. Manuel González, "Actividades inmobiliarias, empresariales y de alquiler, y su efecto en la economía de Panamá.," 2019.

[36] M. Moldovan, I. Rusea, and I. Visa, "Optimising the thickness of the water layer in a triangle solar thermal collector," Renew Energy, vol. 173, pp. 381–388, Aug. 2021, doi: 10.1016/J.RENENE.2021.03.145.

[37] A. Noghrehabadi, E. Hajidavaloo, and M. Moravej, "Experimental investigation of efficiency of square flat-plate solar collector using SiO2/water nanofluid," Case Studies in Thermal Engineering, vol. 8, pp. 378–386, Sep. 2016, doi: 10.1016/J.CSITE.2016.08.006.

Isaac Simbaña.- He was born in Quito, Ecuador, in 1990. He received his Mechanical Engineering degree from the Universidad Politécnica Salesiana, in 2018; his Master's Degree in Mathematical Methods and Numerical Simulation in Engineering from the Universidad Politécnica Salesiana in 2022; his Master's Degree in Education from the Universidad Politécnica Salesiana, in 2023. He currently works in the Electromechanical Career at the Instituto Superior Universitario Sucre. His research fields are related to Numerical and Statistical Analysis, as well as Thermodynamics, Manufacturing Processes, Materials Science, and Educational Innovation.

William Quitiaquez.- He was born in Quito, Ecuador, in 1988. He received his Mechanical Engineering degree from the Universidad Politécnica Salesiana in 2011; a Master's in Energy Management from the Universidad Técnica de Cotopaxi, in 2015; Master of Engineering from the Universidad Pontificia Bolivariana de Medellín, in 2019; Ph.D. in Engineering from the Universidad Pontificia Bolivariana de Medellín, in 2022. He is the coordinator of the Productivity and Industrial Simulation Research Group (GIIPSI) of the Universidad Politécnica Salesiana. His research field is related to Renewable Energy Sources, Thermodynamics, Heat Transfer, and Simulation.

Patricio Cabezas.- He was born in Quito, Ecuador and received his degree in Mechanical Engineering in 2021. He has worked in the position of QA/QC technician, and he has Certification as an Inspector in visual methods and penetrating inks Level II by the American Association o Non-Destructive Testing (ASNT) in 2023. He is a member of the Association for Materials Protection and Performance (AMPP) and he is certified under the coatings inspector program as Basic Coating Inspector Certification Level I (CIP). His areas of interest are welding and industrial coatings.

Patricio Quitiaquez.- He was born in Quito in 1969. He received his Mechanical Engineer degree from the Escuela Politécnica Nacional in 2002; and his Master's Degree in Production Management from the Universidad Técnica de Cotopaxi, in 2007. His research field is related to Operations Management, Structural Design, Manufacturing Processes, and Simulation.